

Dipolar Ordering and Quantum Dynamics of Domain Walls in Mn-12 Acetate

D. A. Garanin and E. M. Chudnovsky

*Department of Physics and Astronomy, Lehman College, City University of New York,
250 Bedford Park Boulevard West, Bronx, New York 10468-1589, U.S.A.*

(Dated: August 17, 2021)

We find that dipolar interactions favor ferromagnetic ordering of elongated crystals of Mn₁₂ Acetate below 0.8 K. Ordered crystals must possess domain walls. Motion of the wall corresponds to a moving front of Landau-Zener transitions between quantum spin levels. Structure and mobility of the wall are computed. The effect is robust with respect to inhomogeneous broadening and decoherence.

PACS numbers: 75.50.Xx, 75.47.-m, 75.60.Ch

I. INTRODUCTION

Molecular magnets exhibit quantum dynamics at the macroscopic level. The best-known expression of such a dynamics is the staircase magnetization curve that one observes on changing the magnetic field.^{1,2,3} The steps occur due to Landau-Zener transitions between crossing quantum spin levels.⁴ It has been previously demonstrated that dipole-dipole interactions in molecular magnets lead to ferro- or antiferromagnetic ordering of spins at low temperature.^{5,6,7,8,9} The Curie temperature as high as 0.9 K was reported in neutron scattering experiments on Mn₁₂ Acetate.⁹ In this paper we re-examine the effect of dipolar interactions in Mn₁₂ within numerical model that treats spin-10 clusters as point magnetic dipoles located at the sites of a body centered tetragonal lattice. We find that elongated crystals must order ferromagnetically below 0.8 K.

It has been noticed in the past¹⁰ that magnetic relaxation in molecular magnets is a collective effect. Indeed, the change of the spin state of one molecule results in the change of the long-range dipolar field acting on other spins. When this change in the local dipolar field causes crossing of spin levels at a certain crystal site, the spin state of the molecule at that site changes as well. Quantum many-body Landau-Zener dynamics of molecular magnets has been intensively studied in recent years by means of Monte Carlo simulations^{11,12,13} and by analytical methods.^{14,15} In this paper we employ analytical model that takes into account both, local spin transitions and the long-range dynamics of the dipolar field. Within such a model it becomes obvious that existing Monte Carlo simulations of collective spin dynamics of molecular magnets have missed an essential feature of that process: Below ordering temperature the relaxation may occur via propagation of a domain wall (DW) separating spin-up and spin-down regions. Unlike domain-wall motion in conventional ferromagnets, the dynamics of the domain wall in a molecular magnet is entirely quantum. It is driven by quantum transitions between spin levels that are crossed in a deterministic manner in space and time by a propagating wave of the dipolar magnetic field. Note that a propagating front of the magnetization reversal has been recently observed in Mn₁₂ crystals and interpreted as magnetic deflagration.^{16,17,18} The latter is

a classical phenomenon equivalent to the flame propagation, with the Zeeman energy playing the role of the chemical energy. Quantum mechanics enters the deflagration problem only through the reduction of the energy barrier near the tunneling resonance. On the contrary, the phenomenon described in this paper has quantum origin. It corresponds to a wave of Landau-Zener transitions generated by dipole-dipole interaction between magnetic molecules in a crystal.

We consider quantum tunneling between two nearly degenerate ground states $|\pm S\rangle$ of magnetic molecules at low temperatures, interacting with each other as magnetic dipoles. The molecules are then effectively described by spin 1/2 instead of spin 10. In the absence of quantum tunneling between $|\pm S\rangle$ these states do not communicate with each other so that any initial distribution of molecules in spin-up and spin-down states will be preserved. The measure of communication between $|\pm S\rangle$ is their tunnel splitting Δ . The effects described in this paper, such as ferromagnetic ordering and motion of domain walls, can be observed only if Δ is sufficiently large. In Mn₁₂ it can be controlled by the transverse magnetic field. Since we are interested in the motion of domain walls, we choose elongated sample in the shape of a long cylinder of length L and radius R , the quantization axis of spins being directed along the z -axis of the cylinder. We restrict our consideration to the states only weakly nonuniform at the lattice scale, so that spins in macroscopic regions are parallel to each other. This can be achieved by either polarizing spins by the external magnetic field or through ferromagnetic order which, as we shall see below, plays an important role at low temperatures where many experiments were performed. We further simplify the problem by ignoring inhomogeneities along the perpendicular axes x and y , so that $\sigma_z \equiv \langle S_z \rangle / S$ depends on z only.

II. THE MODEL

A. The density matrix equation

The effective Hamiltonian of one magnetic molecule at site i within the MFA, taking into account only the two ground states $|\pm S\rangle$ of a molecular magnet at low

temperature, can be formulated in terms of pseudospin (below spin) $\hat{\sigma}$ as

$$\hat{H}_{\text{eff}} = -\frac{1}{2}W\hat{\sigma}_z - \frac{1}{2}\Delta\hat{\sigma}_x. \quad (1)$$

Here $W = 2Sg\mu_B B_z$ is the energy bias that generally depends on time via the total longitudinal field B_z including the external and dipolar fields. Δ is tunnel splitting defined by the uniaxial anisotropy D and the terms in the Hamiltonian that cause tunneling, e.g., transverse field B_\perp . Finally, $\hat{\sigma}_z, \hat{\sigma}_x$ are Pauli matrices. The energy levels of this Hamiltonian for an instantaneous value of W are

$$\varepsilon_\pm = \pm \frac{1}{2}\hbar\omega_0, \quad \omega_0 = \frac{1}{\hbar}\sqrt{W^2 + \Delta^2}, \quad (2)$$

where ω_0 is the corresponding transition frequency.

The density-matrix equation (DME) for the spin in the time-dependent adiabatic basis, formed by the instantaneous eigenstates $|\chi_\pm\rangle$ of \hat{H}_{eff} , has the form

$$\begin{aligned} \frac{d}{dt}\rho_{++} &= (\langle\dot{\chi}_+|\chi_+\rangle + \langle\chi_+|\dot{\chi}_+\rangle)\rho_{++} + \\ &\langle\dot{\chi}_+|\chi_-\rangle\rho_{-+} + \rho_{+-}\langle\chi_-\dot{\chi}_+\rangle - \Gamma_{-+}\rho_{++} + \Gamma_{+-}\rho_{--} \\ \frac{d}{dt}\rho_{+-} &= (\langle\dot{\chi}_+|\chi_+\rangle + \langle\chi_-\dot{\chi}_-\rangle)\rho_{+-} + \rho_{++}\langle\chi_+|\dot{\chi}_-\rangle \\ &+ \langle\dot{\chi}_+|\chi_-\rangle\rho_{--} - \left[i\omega_0 + \frac{1}{2}(\Gamma_{-+} + \Gamma_{+-}) \right] \rho_{+-}, \quad (3) \end{aligned}$$

where Γ_{-+}, Γ_{+-} are up and down relaxation rates for the levels ε_\pm , satisfying the detailed balance condition $\Gamma_{+-} = e^{-\hbar\omega_0/(k_B T)}\Gamma_{-+}$. The elements of the density matrix satisfy $\rho_{++} + \rho_{--} = 1$ and $\rho_{-+} = (\rho_{+-})^*$.

Taking time derivative of the spin expectation value $\sigma = \text{Tr}(\rho\hat{\sigma})$ and using the relation

$$\sigma = (\rho_{+-} + \rho_{-+})\mathbf{e}_x + i(\rho_{+-} - \rho_{-+})\mathbf{e}_y + (\rho_{--} - \rho_{++})\mathbf{e}_z, \quad (4)$$

one finds that in the chosen time-dependent frame the DME describes damped precession of σ about the effective field $\omega_0 + \dot{\theta}\mathbf{e}_y$, where

$$\omega_0 = \frac{1}{\hbar}(\Delta\mathbf{e}_x + W\mathbf{e}_z) \quad (5)$$

and $\cos\theta = W/\sqrt{W^2 + \Delta^2}$ describes the orientation of ω_0 . Switching to the laboratory coordinate frame (which amounts to dropping non-adiabatic term $\dot{\theta}$ in the effective field) one obtains

$$\begin{aligned} \dot{\sigma} &= [\sigma \times \omega_0] \\ &- \frac{\Gamma}{2} \left(\sigma - \frac{\omega_0 \cdot \sigma}{\omega_0^2} \omega_0 \right) - \Gamma \left(\frac{\omega_0 \cdot \sigma}{\omega_0^2} \omega_0 - \sigma \right), \quad (6) \end{aligned}$$

where $\Gamma = \Gamma_{-+} + \Gamma_{+-}$ and σ_0 is the thermal equilibrium value of the pseudospin, corresponding to the instantaneous value and direction of ω_0 . The second term in this equation corresponds to the relaxation of the spin component perpendicular to ω_0 while the third term corresponds to relaxation along ω_0 , the latter being twice as fast as the former.

The equilibrium solution of Eq. (6) has the form

$$\sigma = \sigma_0 = \sigma_0 \frac{\omega_0}{\omega_0}, \quad \sigma_0 = \tanh \frac{\hbar\omega_0}{2k_B T}. \quad (7)$$

Remember that the equations above are written for the spin on a site i , although the index i is not explicitly written for brevity. The equation of motion (6) for spin i couples to those for all other spins j via the magnetostatic contribution in W considered in the next section.

In transverse field B_\perp satisfying $\hbar\omega_0 \ll g\mu_B B_\perp$ the relaxation rate Γ due to direct processes is given by

$$\Gamma = \frac{S^2 \Delta^2 \omega_0 (g\mu_B B_\perp)^2}{12\pi E_t^4} \coth \frac{\hbar\omega_0}{2k_B T}, \quad (8)$$

where $E_t \equiv (\rho v_t^5 \hbar^3)^{1/4}$ is a characteristic energy. For Mn_{12} $E_t/k_B \simeq 150$ K but the factor 1/2 should be introduced in Γ since there is only one transverse sound mode. Usually direct rates are proportional to ω_0^3 but in the case of tunneling there is an additional factor ω_0^{-2} accounting for the decrease of hybridization of the two levels with increasing the energy bias W .

The model formulated above describes the Landau-Zener effect in the case of time-dependent energy bias W that crosses zero, as well as relaxation. In the presence of dipolar coupling this model describes magnetic ordering and domain-wall dynamics. Especially interesting is possible interplay between the DW dynamics and LZ effect that can possibly lead to Landau-Zener fronts. The model can be extended by including heating the sample as the result of spin relaxation. This leads to formation of deflagration fronts if the relaxation rate strongly increases with temperature.

B. The dipolar field

The energy bias W in the equations above at the site i is given by

$$W_i = 2Sg\mu_B (B_z + B_{i,z}^{(D)}) \equiv W_{\text{ext}} + W_i^{(D)}, \quad (9)$$

where B_z is the z component of the external field and $B_{i,z}^{(D)}$ is the dipolar field at site i . The dipolar component of the bias is given by

$$W_i^{(D)} = 2E_D D_{i,zz}, \quad D_{i,zz} \equiv \sum_j \phi_{ij} \sigma_{jz}, \quad (10)$$

where $E_D \equiv (g\mu_B S)^2 / v_0$ is the dipolar energy, v_0 is the unit-cell volume, and

$$\phi_{ij} = v_0 \frac{3(\mathbf{e}_z \cdot \mathbf{n}_{ij})^2 - 1}{r_{ij}^3}, \quad \mathbf{n}_{ij} \equiv \frac{\mathbf{r}_{ij}}{r_{ij}} \quad (11)$$

is the dimensionless dipole-dipole interaction between the spins at sites i and $j \neq i$. The z component of the dipolar field itself is given by

$$B_{i,z}^{(D)} = \frac{Sg\mu_B}{v_0} D_{i,zz}. \quad (12)$$

To calculate the dipolar field, one can introduce a macroscopic sphere of radius r_0 satisfying $v_0^{1/3} \ll r_0 \ll L$ around the site i , where L is the (macroscopic) linear size of the sample. The field from the spins at sites j inside this sphere can be calculated by direct summation over the lattice, whereas the field from the spins outside the sphere can be obtained by integration. The details are given in the Appendix. In particular, for a uniformly magnetized ellipsoid the total result has the form

$$D_{zz} \equiv \sigma_z \sum_j \phi_{ij} = \bar{D}_{zz} \sigma_z, \quad (13)$$

independently of i , where

$$\bar{D}_{zz} = \bar{D}_{zz}^{(\text{sph})} + 4\pi\nu \left(1/3 - n^{(z)}\right) \quad (14)$$

and ν is the number of molecules per unit cell. For the demagnetizing factor one has $n^{(z)} = 0, 1/3$, and 1 for a cylinder, sphere, and disc, respectively. One obtains $\bar{D}_{zz}^{(\text{sph})} = 0$ for a simple cubic lattice, $\bar{D}_{zz}^{(\text{sph})} < 0$ for a tetragonal lattice with $a = b > c$, and $\bar{D}_{zz}^{(\text{sph})} > 0$ for $a = b < c$.

$$E_0 = -(1/2)\bar{D}_{zz}E_D \quad (15)$$

is the dipolar energy per site.

The two best known molecular magnets are Mn_{12} and Fe_8 , both having total spin $S = 10$. Mn_{12} crystalizes in a body-centered tetragonal (bct) lattice with $a = b = 17.319 \text{ \AA}$, $c = 12.388 \text{ \AA}$ (c being the easy axis) and the unit-cell volume $v_0 = abc = 3716 \text{ \AA}^3$, with two molecules per unit cell, $\nu = 2$. Fe_8 has a triclinic lattice with $a = 10.52 \text{ \AA}$ (a being the easy axis), $b = 14.05 \text{ \AA}$, $c = 15.00 \text{ \AA}$, $\alpha = 89.9^\circ$, $\beta = 109.6^\circ$, $\gamma = 109.3^\circ$ and $v_0 = abc \sin \alpha \sin \beta \sin \gamma = 1971 \text{ \AA}^3$. The characteristic dipolar energies thus are $E_D/k_B = 0.0671 \text{ K}$ for Mn_{12} and $E_D/k_B = 0.126 \text{ K}$ for Fe_8 .

For Fe_8 direct numerical calculation yields¹⁴ $\bar{D}_{zz}^{(\text{sph})} = 4.072$, thus for the cylinder Eq. (14) yields $\bar{D}_{zz}^{(\text{cyl})} = 8.261$. Our result $E_0 = -4.131E_D$ for the elongated Fe_8 crystal is in qualitative accord with $E_0 = -4.10E_D$ of Ref. 6.

For Mn_{12} one obtains $\bar{D}_{zz}^{(\text{sph})} = 2.155$ that results in $\bar{D}_{zz}^{(\text{cyl})} = 10.53$ for a cylinder. Then Eq. (12) yields the dipolar field $B_z^{(D)} \simeq 0.0526 \text{ T}$ in an elongated sample. On the top of it, there is a weak ferromagnetic exchange interaction between the neighboring Mn_{12} molecules that creates an effective field 7 G from each neighbor.¹⁹ With 8 nearest neighbors in the bct lattice, this effectively adds 1.12 to \bar{D}_{zz} in the ferromagnetic state. Thus for Mn_{12} one obtains effectively $\bar{D}_{zz}^{(\text{cyl})} \simeq 11.65$.

It can be shown that all other types of ordering have a lower value of \bar{D}_{zz} and thus a higher value of the ground-state energy E_0 for both Mn_{12} and Fe_8 of a cylindrical shape. For Fe_8 the state with ferromagnetically ordered planes alternating in the c direction has $\bar{D}_{zz} = 8.18$, the dipolar field being shape independent. This value is very close to 8.261 for the ferromagnetically ordered cylinder

and it has only slightly higher energy E_0 . The states with ferromagnetic planes alternating in the b direction has $\bar{D}_{zz} = 8.12$, while the state of ferromagnetic chains directed along the a axis and alternating in b and c direction has $\bar{D}_{zz} = 8.01$. One can see that a crystal of Fe_8 cooled in zero field will show a random mixture of different types of ordering. On the other hand, as different kinds of ordered states are separated by energy barriers, prepared ordered states should be robust metastable states. In particular, ferromagnetically ordered state of an elongated Fe_8 crystal, obtained by cooling in the magtic field, should be stable after removing this field at low temperatures.

For Mn_{12} , states with ferromagnetically ordered planes alternating in the a or b directions in *each* sublattice have $\bar{D}_{zz} = 9.480$, independently of the shape and of the exchange interaction. The state with alternating chains directed along the c direction has a very close value $\bar{D}_{zz} = 9.475$. For the two-sublattice antiferromagnetic ordering one obtains $\bar{D}_{zz} = 8.102$. All these values are essentially lower than the dipolar field $\bar{D}_{zz}^{(\text{cyl})} \simeq 11.65$ for a cylinder. Thus one can expect that elongated crystals of Mn_{12} will order ferromagnetically without competition of other states.

On the other hand, for a spherical shape the states with alternating ferromagnetically ordered planes and chains are energetically more favorable for both Fe_8 and Mn_{12} .

For a cylinder magnetized with $\sigma_z = \sigma_z(z)$, the field along the symmetry axis has the form

$$D_{zz}(z) = \nu \int_{-L/2}^{L/2} dz' \frac{2\pi R^2 \sigma_z(z')}{\left[(z' - z)^2 + R^2\right]^{3/2}} - k\sigma_z(z), \quad (16)$$

where

$$k \equiv 8\pi\nu/3 - \bar{D}_{zz}^{(\text{sph})} = 4\pi\nu - \bar{D}_{zz}^{(\text{cyl})} > 0, \quad (17)$$

$k = 14.6$ for Mn_{12} and $k = 4.31$ for Fe_8 . For a uniformly polarized cylinder Eq. (16) yields

$$D_{zz}(z) = 2\pi\nu \left(\frac{z + L/2}{\sqrt{(z + L/2)^2 + R^2}} - \frac{z - L/2}{\sqrt{(z - L/2)^2 + R^2}} \right) \sigma_z - k\sigma_z \quad (18)$$

In the depth of a long cylinder, $L \gg R$, the dipolar field is $D_{zz} = \left(\bar{D}_{zz}^{(\text{sph})} + 4\pi\nu/3\right) \sigma_z$, in accordance with Eq. (14).

At an end of a long cylinder one has $D_{zz} = \left(\bar{D}_{zz}^{(\text{sph})} - 2\pi\nu/3\right) \sigma_z$ that can have the sign opposite to that in the depth of the sample. In particular, for Fe_8 with $\bar{D}_{zz}^{(\text{sph})} = 4.072$ and $\nu = 1$ one has $D_{zz} = 1.98\sigma_z$. Thus a homogeneously magnetized state in zero field is stable. To the contrary, for Mn_{12} with $\bar{D}_{zz}^{(\text{sph})} = 2.155$ and $\nu = 2$ one has $D_{zz} = -2.03\sigma_z$. This means that a homogeneously magnetized state in zero external field is

unstable with respect to domain formation, beginning in the vicinity of the ends of the cylinder. At some point near the end of the crystal the resonance condition $D_{zz}(z) = 0$ is satisfied that leads to spin tunneling and the decay of the initially homogeneously magnetized state.

If there is a domain wall at $z = 0$ ($\sigma_z \rightarrow \sigma_\infty$ for $z \rightarrow -\infty$) in a long cylinder that is narrow in comparison to R , Eq. (16) far from the ends yields

$$D_{zz}(z) = -4\pi\nu \frac{z - z_0}{\sqrt{(z - z_0)^2 + R^2}} \sigma_\infty - k\sigma_z(z). \quad (19)$$

Since the coefficient of the local term is negative, the latter changes in the opposite direction with respect to the first term. This creates three zeros of $D_{zz}(z)$. However, such exotic DWs do not exist, as we will see below. Thermodynamically stable domain walls have only one zero of $D_{zz}(z)$, thus their width at low temperatures is of order R .

III. DIPOLAR ORDERING AND STATIC DOMAIN WALL PROFILE

A. Ferromagnetic ordering

Dipolar field causes ferromagnetic ordering in elongated crystals of molecular magnets that is described within the MFA by the Curie-Weiss equation following from Eqs. (7), (9), and (13). This equation for a homogeneously magnetized sample of an ellipsoidal shape has the form

$$\sigma_z = \frac{W_{\text{ext}} + 2E_D \bar{D}_{zz} \sigma_z}{\hbar\omega_0} \tanh \frac{\hbar\omega_0}{2k_B T}, \quad (20)$$

where $\hbar\omega_0 = \sqrt{(W_{\text{ext}} + 2E_D \bar{D}_{zz} \sigma_z)^2 + \Delta^2}$. This equation is similar to that for the Ising model in a transverse field, here Δ . The Curie temperature satisfies the equation

$$1 = \frac{2E_D \bar{D}_{zz}}{\Delta} \tanh \frac{\Delta}{2k_B T_C}. \quad (21)$$

This equation has a solution only for $\Delta < E_D \bar{D}_{zz}$ as the transverse field tends to suppress the phase transition. In the actual case $\Delta \ll E_D \bar{D}_{zz}$ one obtains

$$T_C = E_D \bar{D}_{zz} / k_B. \quad (22)$$

For a Mn_{12} one has $E_D/k_B \simeq 0.0671$ K. Thus for a cylinder ($\bar{D}_{zz} \simeq 11.65$) Eq. (22) yields $T_C \simeq 0.782$ K. This is close to the value 0.9 K reported in Ref. 9. Note that the MFA does not account for fluctuations that usually lower T_C . However, as we have seen above, for the Mn_{12} cylinder the main contribution to the dipolar field comes from a great number of distant spins, thus the MFA should work well. The small disagreement in T_C can be attributed to approximating magnetic molecules by point dipoles in our calculations.

The equilibrium value of σ_z in zero field below T_C satisfies the equation

$$1 = \frac{2E_D \bar{D}_{zz}}{\hbar\omega_0} \tanh \frac{\hbar\omega_0}{2k_B T}, \quad (23)$$

where $\hbar\omega_0 = \sqrt{(2E_D \bar{D}_{zz} \sigma_z)^2 + \Delta^2}$. In the realistic case $\Delta \ll E_D \bar{D}_{zz}$ not too close to the Curie point one can neglect Δ^2 in $\hbar\omega_0$, then Eq. (23) defining the spin polarization below T_C takes the form

$$\sigma_z = \tanh \frac{E_D \bar{D}_{zz} \sigma_z}{k_B T}. \quad (24)$$

For Mn_{12} the ratio $\Delta / (2E_D \bar{D}_{zz})$ is small. Even for $B_\perp = 5$ T that corresponds to $h_\perp \equiv g\mu_B B_\perp / (2SD) = 0.61$, one has $\Delta/k_B = 0.00166$ K and thus $\Delta / (2E_D \bar{D}_{zz}) \simeq 2.5 \times 10^{-3}$.

B. Static domain wall profile

The magnetization profile $\sigma_z(z)$ in a domain wall joining regions with $\sigma_z = \pm \sigma_\infty = \pm \sigma_z^{\text{eq}}$ in zero field satisfies the equation

$$\sigma_z = \frac{2E_D D_{zz}(z)}{\hbar\omega_0} \tanh \frac{\hbar\omega_0}{2k_B T}, \quad (25)$$

where $\hbar\omega_0 = \sqrt{[2E_D D_{zz}(z)]^2 + \Delta^2}$. Here $D_{zz}(z)$ is given by Eq. (16) that makes Eq. (25) an integral equation. By symmetry, $D_{zz}(z)$ goes through zero in the center of the DW. At very low temperatures, $T \ll \Delta/k_B$, the argument of \tanh is always large, thus Eq. (25) simplifies to

$$\sigma_z = \frac{2E_D D_{zz}(z)}{\sqrt{[2E_D D_{zz}(z)]^2 + \Delta^2}}. \quad (26)$$

In this limit the spin length is nearly constant, $\sigma \simeq 1$, so that $\sigma_x \simeq \sqrt{1 - \sigma_z^2}$. The spin-polarization deficit in the wall is defined by

$$\begin{aligned} 1 - \sigma &= 1 - \tanh \frac{\sqrt{[2E_D D_{zz}(z)]^2 + \Delta^2}}{2k_B T} \\ &\simeq \frac{2k_B T}{\sqrt{[2E_D D_{zz}(z)]^2 + \Delta^2}} \ll 1 \end{aligned} \quad (27)$$

and it reaches the maximum at the DW center. With the help of Eq. (26) one finds

$$1 - \sigma \simeq \frac{2k_B T}{\Delta} \sqrt{1 - \sigma_z^2}. \quad (28)$$

In the opposite limit $\Delta/k_B \ll T$ Eq. (25) simplifies to

$$\sigma_z = \tanh \frac{E_D D_{zz}(z)}{k_B T}. \quad (29)$$

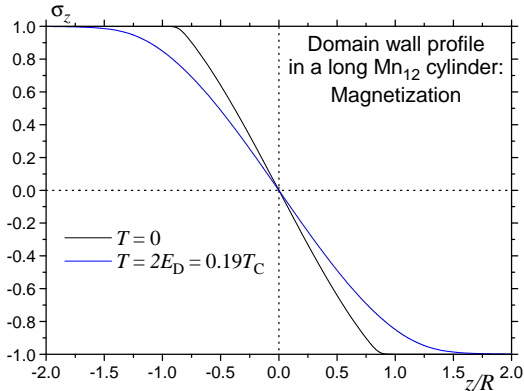


FIG. 1: Magnetization profile of a domain-wall in a Mn_{12} cylinder at two different temperatures.

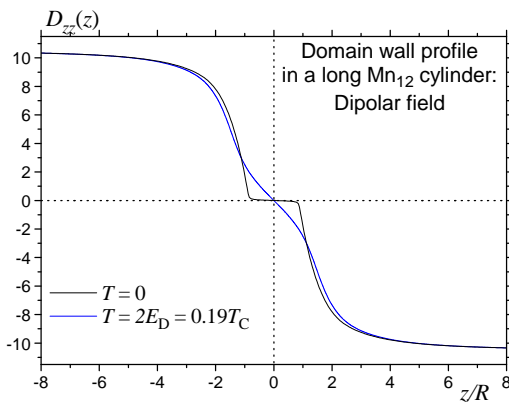


FIG. 2: Dipolar-field profile of a domain-wall in a Mn_{12} cylinder at two different temperatures.

The transverse spin component in this case is given by

$$\sigma_x = \frac{\Delta}{2E_D D_{zz}(z)} \tanh \frac{E_D D_{zz}(z)}{k_B T}, \quad (30)$$

and $\sigma_x = \Delta/(2k_B T) \ll 1$ at the center of the DW. For Mn_{12} σ_x is very small except of very low temperatures and very large transverse fields. Such a domain wall is the linear (Ising-like) domain wall found in ferromagnets in a narrow temperature range below T_C ,^{20,21,22,23} as well as in the low-temperature strong-anisotropy ferromagnet GdCl_3 .²⁴ Absence of a strong short-range exchange interaction in molecular magnets makes domain walls linear practically in the whole range below T_C .

For Mn_{12} the splitting Δ is typically so small that one can consider the limit $T \rightarrow 0$ of Eq. (29). Then three regions arise: (i) left from the DW where $\sigma_z = 1$ and the argument of \tanh is infinite, that is, $D_{zz}(z) > 0$; (ii) inside the DW where $|\sigma_z| < 1$ and thus $D_{zz}(z) = 0$; right from the DW where $\sigma_z = -1$ and $D_{zz}(z) < 0$. Using Eq. (16) with $L = \infty$ one obtains the integral equation for

the nontrivial region inside the DW centered at $z = 0$:

$$0 = \nu \int_{-l}^l dz' \frac{2\pi R^2 \sigma_z(z')}{[(z' - z)^2 + R^2]^{3/2}} - k\sigma_z(z) - 2\pi\nu \left(\frac{z-l}{\sqrt{(z-l)^2 + R^2}} + \frac{z+l}{\sqrt{(z+l)^2 + R^2}} \right), \quad (31)$$

where l is the DW width that should follow from the equation above and the boundary conditions are $\sigma_z(\pm l) = \mp 1$. One can see that still in for $T \rightarrow 0$ the DW profile results from an essentially integral equation that does not have a general analytical solution, although analytical solutions in limiting cases do exist. Rewriting Eq. (31) in terms of $\tilde{z} \equiv z/R$, one can show that the DW profiles scales with the cylinder radius R , i.e., $l \sim R$.

Numerical solution using relaxation to the equilibrium described by Eq. (25) with proper boundary conditions at the ends of a long Mn_{12} cylinder is shown in Figs. 1 and 2. One can see that at $T = 0$ the magnetization profile turns to ± 1 beyond the region of the DW of the length $l \sim R$, in accordance with Eq. (31). At finite temperatures the solution for $\sigma_z(z)$ is more resembling a tanh. The DW width l increases with temperature and diverges at T_C . The solution for the dipolar field in Fig. 2 shows that $D_{zz}(z) \rightarrow 0$ at $T \rightarrow 0$ inside the domain wall while it is approaching the asymptotic value ± 11.65 in the domains. At finite temperatures the dependence $D_{zz}(z)$ smoothens out. Overall the region of inhomogeneity of the dipolar field is broader than that of the magnetization.

The DW width l can be defined as a slope

$$l^{-1} = \frac{1}{\sigma_\infty} \left. \frac{d\sigma_z}{dz} \right|_{z=0}. \quad (32)$$

Some results for l can be obtained analytically. At $T \ll T_C$, assuming that the magnetization profile in the DW is close to the piece-wise linear, one obtains from Eq. (29)

$$\begin{aligned} \frac{l_{LT}}{R} &= \left[(4\pi\nu)^2 \left(\frac{k_B T}{E_D} + k \right)^{-2} - 1 \right]^{-1/2} \\ &= \frac{4\pi\nu E_D + T - T_C}{\sqrt{(T_C - T)(8\pi\nu E_D + T - T_C)}}, \end{aligned} \quad (33)$$

in a qualitative agreement with numerical results in Fig. 3. At $T \rightarrow T_C$ the solution of Eq. (29) is

$$\sigma_z(z) = \sigma_\infty \tanh \frac{z}{l_{HT}}, \quad (34)$$

where $\sigma_\infty = \sqrt{3}(T_C/T - 1)^{1/2}$ and l_{HT} satisfies

$$l_{HT}^2 = l_{LT}^2 \ln \frac{l_{HT}^2}{2R^2} \quad (35)$$

with l_{LT} of Eq. (33) diverging as

$$\frac{l_{LT}}{R} = \sqrt{\frac{2\pi E_D}{k_B(T_C - T)}}. \quad (36)$$

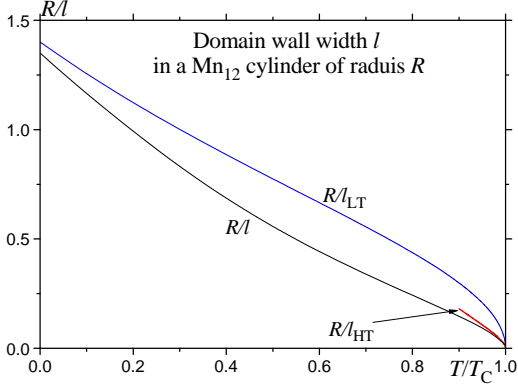


FIG. 3: Temperature dependence of the DW width l and its low- and high-temperature forms in a Mn_{12} cylinder.

Temperature dependence of the approximations l_{LT} and l_{HT} , together with numerical result for the domain wall width l , is shown in Fig. 3.

IV. DOMAIN-WALL DYNAMICS

In the sequel we will be mostly interested in the motion of domain walls with a small speed, induced by a small external bias B_z . In this case the system does not deviate much from the equilibrium. In this case domain walls in a sufficiently long sample are stationarily moving with a speed v_{DW} that is proportional to the bias field. This relation has the form

$$v_{DW} = \mu_{DW} B_z, \quad (37)$$

where μ_{DW} is the *linear mobility* of the DW. At high values of B_z the dependence $v_{DW}(H_z)$ becomes nonlinear. The linear mobility μ_{DW} can be calculated using the *static* DW profile discussed above with the help of the energy balance argument. To this end, the LLB equation (6) should be transformed into a special form near the equilibrium.

A. Landau-Lifshitz-Bloch equation near equilibrium

One can project relaxation terms in Eq. (6) on the directions parallel and perpendicular to σ using

$$\mathbf{R} = \frac{(\sigma \cdot \mathbf{R}) \sigma}{\sigma^2} - \frac{[\sigma \times [\sigma \times \mathbf{R}]]}{\sigma^2}. \quad (38)$$

This results in a Landau-Lifshitz-Bloch (LLB) equation

$$\begin{aligned} \dot{\sigma} &= [\sigma \times \omega_0] \\ &+ \Gamma \left[\frac{\omega_0 \cdot \sigma}{\omega_0 \sigma} \left(\frac{\sigma_0}{\sigma} - 1 \right) - \frac{1}{2} \left(1 - \frac{\omega_0 \cdot \sigma}{\omega_0 \sigma} \right)^2 \right] \sigma \\ &- \frac{\Gamma}{2} \left(2\sigma_0 - \frac{\omega_0 \cdot \sigma}{\omega_0} \right) \frac{[\sigma \times [\sigma \times \omega_0]]}{\omega_0 \sigma^2}. \end{aligned} \quad (39)$$

Here, in contrast to ferromagnets where $\sigma \cong 1$ is enforced by a strong exchange, σ can essentially deviate from 1 because of the first relaxation term. Close to equilibrium vectors ω_0 and σ are nearly collinear, thus $\omega_0 \cdot \sigma \cong \omega_0 \sigma$ holds up to quadratic terms in small deviations, whereas σ is close to σ_0 . Thus the equation above simplifies to

$$\dot{\sigma} = [\sigma \times \omega_0] + \Gamma \left(\frac{\sigma_0}{\sigma} - 1 \right) \sigma - \frac{\Gamma}{2} \frac{[\sigma \times [\sigma \times \omega_0]]}{\sigma \omega_0}. \quad (40)$$

Note that σ_0 is formally defined by Eq. (7) and it is a function of ω_0 that can depend on time. Thus, in general, σ_0 corresponds not to a true equilibrium but to an instantaneous equilibrium to which the system tends. If the state of the system, as well as the instantaneous equilibrium, is close to a true equilibrium, one can approximately express ω_0 through σ and small $\dot{\sigma}$ that has an important application. First, multiplying Eq. (40) by σ one obtains the relation

$$\sigma_0 = \sigma + \frac{1}{\Gamma} \frac{(\sigma \cdot \dot{\sigma})}{\sigma}. \quad (41)$$

Second, using $\omega_0 \cdot \sigma \cong \omega_0 \sigma$ one can rewrite Eq. (40) in the form

$$\dot{\sigma} = [\sigma \times \omega_0] + \Gamma \left(\frac{\sigma_0}{\sigma} - 1 \right) \sigma - \frac{\Gamma}{2} \sigma + \frac{\Gamma}{2} \frac{\sigma}{\omega_0} \omega_0. \quad (42)$$

From the latter follows

$$[\sigma \times \dot{\sigma}] = \sigma \omega_0 \sigma - \omega_0 \sigma^2 + \frac{\Gamma}{2} \frac{\sigma}{\omega_0} [\sigma \times \omega_0]. \quad (43)$$

Eliminating $[\sigma \times \omega_0]$ and using Eq. (41), one obtains

$$\omega_0 = \omega_0 \frac{\sigma}{\sigma} - \frac{\omega_0^2}{\omega_0^2 + \Gamma^2/4} \frac{[\sigma \times \dot{\sigma}]}{\sigma^2} - \frac{\omega_0 \Gamma/2}{\omega_0^2 + \Gamma^2/4} \frac{[\sigma \times [\sigma \times \dot{\sigma}]]}{\sigma^3}. \quad (44)$$

Here the scalar ω_0 can be found from Eqs. (7) and (41):

$$\begin{aligned} \omega_0 &= \frac{2k_B T}{\hbar} \operatorname{arctanh}(\sigma_0) \\ &\cong \frac{2k_B T}{\hbar} \operatorname{arctanh} \left(\sigma + \frac{1}{\Gamma} \frac{(\sigma \cdot \dot{\sigma})}{\sigma} \right) \\ &\cong \frac{2k_B T}{\hbar} \operatorname{arctanh}(\sigma) + \frac{2k_B T}{\hbar \Gamma} \frac{\dot{\sigma}}{1 - \sigma^2}. \end{aligned} \quad (45)$$

The $\dot{\sigma}$ correction here should be taken into account in the first term of Eq. (44).

B. Linear mobility of domain walls

The time derivative of the magnetic energy of the sample per unit cross-sectional area due to dissipation has the form

$$\dot{U} = - \int_{-\infty}^{\infty} dz \hbar \omega_0(z) \cdot \dot{\sigma}(z). \quad (46)$$

On the other hand, motion of the DW results in the change of the energy of the spins in the external field

at the rate $-\sigma_\infty W_{\text{ext}} v_{\text{DW}}$, where $\sigma_\infty > 0$ is the spin polarization in domains and W_{ext} is given by Eq. (9). Equating this rate to Eq. (46), one obtains the energy balance relation

$$\sigma_\infty W_{\text{ext}} v_{\text{DW}} = \int_{-\infty}^{\infty} dz \hbar \omega_0(z) \cdot \dot{\boldsymbol{\sigma}}(z). \quad (47)$$

This relation allows one to obtain the linear mobility of a domain wall as an integral over the static DW profile without solving a complicated problem of dynamical corrections to this profile. To find the linear mobility, one has to express $\omega_0(z)$ through $\dot{\boldsymbol{\sigma}}(z)$ using Eq. (44) that yields

$$\omega_0 \cdot \dot{\boldsymbol{\sigma}} = \omega_0 \frac{\boldsymbol{\sigma} \cdot \dot{\boldsymbol{\sigma}}}{\sigma} + \frac{\omega_0 \Gamma / 2}{\omega_0^2 + \Gamma^2 / 4} \frac{\sigma^2 \dot{\boldsymbol{\sigma}}^2 - (\boldsymbol{\sigma} \cdot \dot{\boldsymbol{\sigma}})^2}{\sigma^3}. \quad (48)$$

After that one has to use the fact that for a domain wall stationarily moving in the positive z direction, all quantities depend on the combined space-like argument $\xi = z - v_{\text{DW}} t$, so that

$$\dot{\boldsymbol{\sigma}} = -v_{\text{DW}} d\boldsymbol{\sigma} / dz. \quad (49)$$

Using Eq. (45), one obtains the energy balance equation in the form

$$\begin{aligned} & \sigma_\infty W_{\text{ext}} \\ &= \int_{-\infty}^{\infty} dz \left\{ \left(2k_{\text{B}} T \operatorname{arctanh}(\sigma) + \frac{2k_{\text{B}} T}{\Gamma} \frac{v_{\text{DW}}}{1 - \sigma^2} \frac{d\sigma}{dz} \right) \right. \\ & \quad \times \left(\frac{\boldsymbol{\sigma} \cdot d\boldsymbol{\sigma}}{\sigma} + \frac{\hbar v_{\text{DW}} \lambda}{\operatorname{arctanh}(\sigma)} \left[1 + \frac{\lambda^2 / 4}{\operatorname{arctanh}^2(\sigma)} \right]^{-1} \right. \\ & \quad \left. \left. \times \left[\frac{1}{\sigma} \left(\frac{d\boldsymbol{\sigma}}{dz} \right)^2 - \frac{1}{\sigma^3} \left(\boldsymbol{\sigma} \cdot \frac{d\boldsymbol{\sigma}}{dz} \right)^2 \right] \right\}, \quad (50) \end{aligned}$$

where

$$\lambda \equiv \frac{\hbar \Gamma}{2k_{\text{B}} T}. \quad (51)$$

Here the first term in the rhs can be easily integrated and gives a zero contribution. Thus the rhs of Eq. (47) becomes proportional to v_{DW}^2 . This is very fortunate since now one does not have to take into account deviations from the static DW profile. In all practical cases the inequality $\lambda \ll 1$ is strongly satisfied, thus one can replace $[\dots]^{-1} \Rightarrow 1$. After that for the DW speed in the linear regime one obtains

$$v_{\text{DW}} = \frac{\sigma_\infty W_{\text{ext}}}{2k_{\text{B}} T} v_* = \frac{S \sigma_\infty g \mu_{\text{B}} B_z}{k_{\text{B}} T} v_*, \quad (52)$$

where v_* is the characteristic speed defined by

$$\begin{aligned} v_*^{-1} &= \int_{-\infty}^{\infty} dz \frac{1}{\Gamma} \left\{ \frac{1}{1 - \sigma^2} \left(\frac{d\sigma}{dz} \right)^2 \right. \\ & \quad \left. + \frac{\lambda^2 / 2}{\sigma \operatorname{arctanh}(\sigma)} \left[\left(\frac{d\boldsymbol{\sigma}}{dz} \right)^2 - \left(\frac{d\sigma}{dz} \right)^2 \right] \right\}, \quad (53) \end{aligned}$$

that resembles the expression for ferromagnets.^{22,23,24,25,26} Note that Γ is not a constant and it has to be kept in the integrand. One can see that if $\sigma \rightarrow 1$ in the domain wall, as is usually supposed to be the case in ferromagnets, then $d\sigma/dz \rightarrow 0$, only the second term makes a contribution, and $\mu_{\text{DW}} \propto 1/\Gamma$. However, if σ only slightly deviates from 1, then because of the very small λ the second term becomes irrelevant and one obtains $\mu_{\text{DW}} \propto \Gamma$ from the first term. For the linear (Ising-like) domain wall, $\boldsymbol{\sigma} = \sigma_z \mathbf{e}_z$, the expression in the square brackets in second term of Eq. (53) disappears. This is the case for Mn₁₂ except for very large transverse fields and very low temperatures.

The crossover between the two different types of the mobility behavior occurs in the low-temperature range $T \ll \Delta/k_{\text{B}}$, where the deviation of σ from 1 is small and given by Eq. (28). Here in Eq. (53) one can simplify

$$\begin{aligned} 1 - \sigma^2 &\cong 2(1 - \sigma) \cong \frac{4k_{\text{B}} T}{\Delta} \sqrt{1 - \sigma_z^2} \\ \left(\frac{d\sigma}{dz} \right)^2 &\cong \left(\frac{4k_{\text{B}} T}{\Delta} \right)^2 \frac{\sigma_z^2}{1 - \sigma_z^2} \left(\frac{d\sigma_z}{dz} \right)^2 \\ \left(\frac{d\boldsymbol{\sigma}}{dz} \right)^2 &= \left(\frac{d\sigma_z}{dz} \right)^2 + \left(\frac{d\sigma_x}{dz} \right)^2 \cong \left(\frac{d\sigma_z}{dz} \right)^2 \\ \operatorname{arctanh}(\sigma) &\cong \frac{1}{2} \ln \frac{2}{1 - \sigma} \\ &\cong \frac{1}{2} \ln \left(\frac{\Delta}{2k_{\text{B}} T} (1 - \sigma_z^2)^{-1/2} \right). \quad (54) \end{aligned}$$

This yields

$$\begin{aligned} v_*^{-1} &= \int_{-\infty}^{\infty} dz \frac{1}{\Gamma} \left\{ \frac{4k_{\text{B}} T}{\Delta} \frac{\sigma_z^2}{(1 - \sigma_z^2)^{3/2}} \right. \\ & \quad \left. + \frac{\lambda^2}{\ln \left(\frac{\Delta}{2k_{\text{B}} T} (1 - \sigma_z^2)^{-1/2} \right)} \right\} \left(\frac{d\sigma_z}{dz} \right)^2. \quad (55) \end{aligned}$$

One can see that the second term dominates and the DW mobility has the form $\mu_{\text{DW}} \propto 1/\Gamma$ only at extremely low temperatures,

$$T \lesssim \frac{\Delta}{k_{\text{B}}} \left(\frac{\hbar \Gamma}{\Delta} \right)^{2/3}, \quad (56)$$

up to the log term. In most region one has $\mu_{\text{DW}} \propto \Gamma$.

For Mn₁₂ in the typical case $\Delta \ll E_{\text{D}}$ the DW is Ising-like, and one should use the first term of Eq. (53), where σ_x and σ_y are negligibly small, so that in Eq. (52) one has

$$v_*^{-1} = \int_{-\infty}^{\infty} dz \frac{1}{\Gamma} \frac{1}{1 - \sigma_z^2} \left(\frac{d\sigma_z}{dz} \right)^2. \quad (57)$$

In the case of the unspecified relaxation rate Γ that is considered as a constant instead of Eq. (52) one obtains

$$v_{\text{DW}} = \frac{\sigma_\infty W_{\text{ext}}}{k_{\text{B}} T} \Gamma v_* \quad (58)$$

with

$$l_*^{-1} = \int_{-\infty}^{\infty} dz \frac{1}{1 - \sigma_z^2} \left(\frac{d\sigma_z}{dz} \right)^2. \quad (59)$$

At $T \ll T_C$ according to Eq. (31) one has $l_* \sim R$ independent of E_D with a coefficient dependent only on the lattice structure. Thus obtains $\mu_{DW} \propto 1/T$ at low temperatures. In this case numerical calculation yields μ_{DW} diverging both at $T \rightarrow 0$ and $T \rightarrow T_C$ and having a minimum at about $0.25T_C$. One can improve the numerical procedure eliminating division 0/0 in domains at $T \rightarrow 0$ using Eq. (29) and

$$\frac{1}{1 - \sigma_z^2} \frac{d\sigma_z}{dz} = \frac{d}{dz} \operatorname{arctanh}(\sigma_z). \quad (60)$$

This yields

$$l_*^{-1} = \frac{E_D}{k_B T} \int_{-\infty}^{\infty} dz \frac{d\sigma_z}{dz} \frac{dD_{zz}}{dz}. \quad (61)$$

This expression is very convenient since at low temperatures $D_{zz} \sim k_B T / E_D$ inside the DW that makes no computational problems. The non-monotonic dependence of v_{DW} on temperature should be taken with caution, however, because it is related to our assumption that Γ is a constant.

For Γ given by Eq. (8) is intimately interwoven with the rest of the mobility formula. Using Eq. (25) in the form

$$\sigma_z = \frac{W(z)}{\hbar\omega_0} \tanh \frac{\hbar\omega_0}{2k_B T}, \quad (62)$$

one can transform Eq. (8) into the form

$$\Gamma = \frac{S^2 \Delta^2 (g\mu_B B_{\perp})^2}{12\pi E_t^4} \frac{W(z)}{\hbar\sigma_z(z)}. \quad (63)$$

eliminating $W(z)$ with the use of Eq. (29) one obtains

$$\Gamma = \frac{S^2 \Delta^2 (g\mu_B B_{\perp})^2}{12\pi E_t^4} \frac{2k_B T}{\hbar} \frac{\operatorname{arctanh}(\sigma_z)}{\sigma_z}. \quad (64)$$

Now Eq. (52) can be rewritten as

$$v_{DW} = 2\sigma_{\infty} \Gamma_0^{(\text{ext})} l_*, \quad (65)$$

where

$$\Gamma_0^{(\text{ext})} \equiv \frac{S^2 \Delta^2 (W_{\text{ext}}/\hbar) (g\mu_B B_{\perp})^2}{12\pi E_t^4} \quad (66)$$

is the prefactor in Eq. (8) with $\hbar\omega_0 \Rightarrow W_{\text{ext}}$ and l_* is a characteristic length defined by

$$l_*^{-1} = \int_{-\infty}^{\infty} dz \frac{\sigma_z}{\operatorname{arctanh}(\sigma_z)} \frac{1}{1 - \sigma_z^2} \left(\frac{d\sigma_z}{dz} \right)^2. \quad (67)$$

Similarly to Eq. (57) with $\Gamma \rightarrow 1$, this integral is finite at $T \rightarrow 0$. To improve its numerical convergence at low

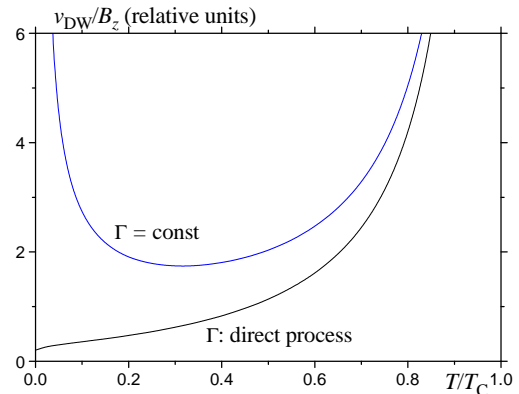


FIG. 4: Temperature dependences of the DW mobility in the cases of $\Gamma = \text{const}$ and of Γ due to the direct phonon processes.

temperatures, one can rewrite it as

$$\begin{aligned} l_*^{-1} &= \int_{-\infty}^{\infty} dz \frac{\sigma_z}{\operatorname{arctanh}(\sigma_z)} \frac{d\sigma_z}{dz} \frac{d\operatorname{arctanh}(\sigma_z)}{dz} \\ &= \int_{-\infty}^{\infty} dz \frac{\sigma_z}{D_{zz}} \frac{d\sigma_z}{dz} \frac{dD_{zz}}{dz}. \end{aligned} \quad (68)$$

Again, at low temperatures $l_* \sim R$ with a coefficient depending only on the lattice structure, c.f. Eq. (61).

Numerical results for temperature dependence of the velocity for $\Gamma = \text{const}$ and for Γ given by a direct phonon process in a transverse magnetic field²⁷ are shown in Fig. 4.

More generally, one can consider the relaxation rate of the form

$$\Gamma = A (\hbar\omega_0)^n \coth \frac{\hbar\omega_0}{2k_B T}, \quad (69)$$

where $A = \text{const}$ at low temperatures. In the case $\Delta \ll E_D$ one has $\hbar\omega_0 \cong W(z)$, then with the help of Eq. (29) one can rewrite Γ as

$$\Gamma = A (2k_B T \operatorname{arctanh}(\sigma_z))^n \frac{1}{\sigma_z}. \quad (70)$$

V. DISCUSSION

We have demonstrated that elongated crystal of magnetic dipoles arranged in a body centered tetragonal lattice should exhibit ferromagnetic ordering. For Mn_{12} Acetate the corresponding Curie temperature computed within mean-field model is about 0.8 K, which is close to the ordering temperature 0.9 K reported in recent neutron scattering experiments.⁹ Other magnetic phases are separated from the ferromagnetic phase by a large energy gap, thus making ferromagnetism in Mn_{12} not difficult to observe. This suggests that the analysis of all previous data on Mn_{12} Acetate that were taken below 0.8 K should be re-examined for possible effects of ferromagnetic order.

Dipolar-ordered crystals of molecular magnets should possess domain walls. In a long crystal of length L and

radius $R \ll L$, the typical width of the domain wall is of order R . When a small bias magnetic field B_z is applied, the domain wall moves at a speed $v_{\text{DW}} \sim [Sg\mu_{\text{B}}B_z/(k_{\text{B}}T)]\langle\Gamma\rangle R$, where $\langle\Gamma\rangle$ is the average spin relaxation rate. At, e.g., $S = 10$, $B_z = 0.1$ T, $T = 1$ K, and $R = 1$ mm, this gives $v_{\text{DW}} \sim 1$ m/s for $\langle\Gamma\rangle = 10^3$ s $^{-1}$ and $v_{\text{DW}} \sim 10^3$ m/s for $\langle\Gamma\rangle = 10^6$ s $^{-1}$. It should be emphasized that contrary to superradiance and laser effects in molecular magnets,^{28,29} quantum dynamics of domain walls is robust with respect to inhomogeneous broadening of spin levels and phase decoherence of spin states. Crossing of spin levels due to a moving front of dipolar field is sufficient for the effect to exist. Neither very narrow spin levels nor phase coherence of spins in the domain wall are required. We, therefore, believe that this effect should not be difficult to observe in molecular magnets.

Our conclusion that low-temperature ferromagnetic phase is unstable against division into domains may seem to contradict experiments on Mn₁₂ in which, at low temperature, the crystal was shown to maintain finite magnetization in a zero field for a very long time. This apparent contradiction becomes resolved if one notices that in the zero-temperature limit any evolution of the magnetic state of the Mn₁₂ crystal can only occur through quantum tunneling between spin levels. The measure of this tunneling is the splitting Δ which for low lying spin-levels is negligibly small in zero field. To increase Δ one should apply transverse magnetic field. Note that some evidence that transverse field is needed to achieve local ferromagnetic order was obtained in Ref. 9. In the absence of the longitudinal field, the existence of the global ferromagnetic order would be hindered by the presence of domain walls. One would need local measurements of the sample to directly confirm ferromagnetic order below the Curie temperature. However, in the presence of sufficient transverse field, a relatively weak longitudinal field of the order of the dipolar field should be able to drive the domain walls out, thus resulting in the uniform magnetization. Another simple experiment can be conducted to observe the domain wall entering the crystal. First the crystal should be uniformly magnetized by a strong longitudinal field. Then the longitudinal field should be switched off and a sufficient transverse field should be turned on. Finally, the compensating longitudinal field should be applied. As soon as the resonant condition is achieved, the domain wall should enter the crystal, resulting in the drastic change of the magnetization. Some of these effects must have been already observed in Mn₁₂ crystals but attributed to resonant quantum flipping of magnetic molecules at random sites, instead of coherent motion of domain walls.

The motion of a domain wall should not be confused with magnetic deflagration.^{16,17,18} The latter is also characterized by a moving front that separates regions with opposite magnetization. However, while deflagration is driven by the release of heat due to a strong field bias, the motion of a domain wall is driven by Landau-Zener transitions in a relatively small bias. In experiment, the two effects can be easily distinguished from each other if

one notices that the mobility of the domain wall depends strongly on the transverse field while deflagration must have little dependence on the transverse field.

In the Introduction it was pointed out that domain walls in elongated crystals of molecular magnets are propagating waves of Landau-Zener transitions. The tunneling and relaxational dynamics of this process is described by the density-matrix equation (3) that has a form of the equation of motion for the magnetization, Eq. (6) in the two-state $|\pm S\rangle$ approximation. The energy sweep in the LZ effect is due to the change of the dipolar field created by quantum spin transitions $|S\rangle \rightleftharpoons |-S\rangle$ in the moving front. Thus, in contrast to the standard LZ effect with externally controlled time-linear sweep, the LZ effect considered here includes a *self-consistent* sweep that turns out to be time nonlinear. Indeed, the spatial profile of the dipolar field in the DW in Fig. 2 is strongly nonlinear at low temperatures. As the domain wall moves, a time-nonlinear sweep is generated. LZ effect with time-nonlinear sweeps generated by interaction between two-level systems have been studied in Ref. 30. It was shown that if the time dependence $W(t)$ becomes steeper near the resonance, the staying probability P increases, whereas in the opposite case the transition probability $1 - P$ increases. Sweeps that become flat near the resonance lead to a nearly complete transition, see, e.g., Fig. 7 of Ref. 30. This is also the case for the sweep corresponding to the $T \rightarrow 0$ curve in Fig. 2. In this case the LZ transition is complete, $P = 0$, that is exactly what should be for a moving DW. Externally controlled sweeps leading to a complete transition have been studied in Ref. 31. The case of moving domain walls is another realization of the full-transition Landau-Zener effect.

Finally we would like to comment on the square root of time magnetic relaxation observed in Mn-12 at low temperature. Existing theoretical works attempted to explain this behavior by flips of molecular spins at random sites of the crystal.^{11,12,13} They missed the fact that the low-temperature phase of Mn₁₂ Acetate is ferromagnetic. Relaxation in the ferromagnetic phase must be determined by the motion of domain walls. Within such picture the square root relaxation may have simple explanation through random walk of the domain wall. If the wall moves randomly at a constant rate to the right or to the left, the resulting displacement and, thus, the change in the magnetization should be proportional to the square root of the number of steps, that is, to the square root of time. Such random walk may be thermal or it may be caused by the adjustment of the domain wall to local solvent disorder or to local hyperfine fields.

Acknowledgements

D. G. would like to acknowledge stimulating discussions with Andrew Kent and Grégoire de Loubens, as well as to thank Kyungwha Park and Chris Beedle for the information on the crystal structure of Mn₁₂ Acetate and Wolfgang Wernsdorfer for the information on the crystal structure of Fe₈. This work has been supported

by the NSF Grant No. DMR-0703639.

APPENDIX A: CALCULATION OF THE DIPOLAR FIELD IN A CRYSTAL LATTICE

The dipolar field $\mathbf{B}_i^{(D)}$ created on the lattice site i by all other spins, $j \neq i$, aligned along the z axis can be written in the form

$$\mathbf{B}_i^{(D)} = \frac{Sg\mu_B}{v_0} \mathbf{D}_{i,z} \quad (\text{A1})$$

with the dimensionless vector $\mathbf{D}_{i,z}$ given by

$$\mathbf{D}_{i,z} \equiv \sum_j \phi_{ij} \sigma_{jz}. \quad (\text{A2})$$

Here σ is the Pauli matrix and

$$\phi_{ij} = v_0 \frac{3\mathbf{n}_{ij}(\mathbf{e}_z \cdot \mathbf{n}_{ij}) - \mathbf{e}_z}{r_{ij}^3}, \quad \mathbf{n}_{ij} \equiv \frac{\mathbf{r}_{ij}}{r_{ij}} \quad (\text{A3})$$

with v_0 being the unit-cell volume. As said above, $\mathbf{D}_{i,z}$ of Eq. (A1) can be represented as a sum of the contributions from the molecules inside and outside the sphere r_0 around the site i satisfying $v_0^{1/3} \ll r_0 \ll L$, where L is the (macroscopic) linear size of the sample. The field from the spins at sites j inside this sphere r_0 can be calculated by direct summation over the lattice, whereas the field from the spins outside the sphere can be obtained by integration. Replacing the index i by the argument \mathbf{r} , one can write

$$\mathbf{D}_z(\mathbf{r}) = \mathbf{D}_z^{(\text{sph})}(\mathbf{r}) + \mathbf{D}'_z(\mathbf{r}), \quad (\text{A4})$$

where

$$\mathbf{D}_z^{(\text{sph})}(\mathbf{r}) \cong \bar{D}_z^{(\text{sph})} \sigma_z(\mathbf{r}) \mathbf{e}_z \quad (\text{A5})$$

and

$$\mathbf{D}'_z(\mathbf{r}) = \frac{\nu}{v_0} \int_{|\mathbf{r}-\mathbf{r}'|>r_0} d^3r' \phi(\mathbf{r}-\mathbf{r}') \sigma_z(\mathbf{r}'). \quad (\text{A6})$$

In Eq. (A5) it is assumed that the change of $\sigma_z(\mathbf{r})$ inside the sphere r_0 is negligible. $\bar{D}_z^{(\text{sph})}$ is a constant depending on the lattice structure. In Eq. (A6) ν is the number of molecules per unit cell,

$$\phi(\mathbf{r}) = v_0 \frac{3\mathbf{n}_r(\mathbf{e}_z \cdot \mathbf{n}_r) - \mathbf{e}_z}{r^3} = v_0 \text{rot} \frac{[\mathbf{e}_z \times \mathbf{n}_r]}{r^2}, \quad (\text{A7})$$

and $\mathbf{n}_r \equiv \mathbf{r}/r$. In the main part of the paper one needs only the z component of the vector \mathbf{D}_z , i.e., D_{zz} .

Using the integral formula

$$\int_V dV \text{rot} \mathbf{F} = \int_S d\mathbf{S} \times \mathbf{F} \quad (\text{A8})$$

and the relation

$$\text{rot}[f\mathbf{A}] = [\nabla f \times \mathbf{A}] + f \text{rot} \mathbf{A}, \quad (\text{A9})$$

one can rewrite Eq. (A6) as

$$\begin{aligned} \mathbf{D}'_z(\mathbf{r}) = & \int_S d\mathbf{S}' \times \sigma_z(\mathbf{r}') \frac{[\mathbf{e}_z \times (\mathbf{r}' - \mathbf{r})]}{|\mathbf{r}' - \mathbf{r}|^3} \\ & - \int_{|\mathbf{r}-\mathbf{r}'|>r_0} d^3r' \nabla \sigma_z(\mathbf{r}') \times \frac{[\mathbf{e}_z \times (\mathbf{r}' - \mathbf{r})]}{|\mathbf{r}' - \mathbf{r}|^3} \\ & - \int_{S_{r_0}} d\mathbf{S}' \times \sigma_z(\mathbf{r}') \frac{[\mathbf{e}_z \times (\mathbf{r}' - \mathbf{r})]}{|\mathbf{r}' - \mathbf{r}|^3}. \end{aligned} \quad (\text{A10})$$

For a flat domain wall with

$$\nabla \sigma_z(\mathbf{r}') = \frac{d\sigma_z(z')}{dz'} \mathbf{e}_z \quad (\text{A11})$$

the second term in Eq. (A10) is zero. In this case one has

$$\mathbf{D}'_z(\mathbf{r}) = \nu \int_S d\mathbf{S}' \times \sigma_z(\mathbf{r}') \frac{[\mathbf{e}_z \times (\mathbf{r}' - \mathbf{r})]}{|\mathbf{r}' - \mathbf{r}|^3} - \frac{8\pi\nu}{3} \sigma_z(\mathbf{r}) \mathbf{e}_z, \quad (\text{A12})$$

where the integral is taken over the surface of the sample, the vector $d\mathbf{S}'$ is directed outwards, and the last term is the integral over the sphere r_0 , taken with $\sigma_z(\mathbf{r}') \Rightarrow \sigma_z(\mathbf{r})$. The first term in Eq. (A12), multiplied by $g\mu_B S/v_0$, yields the *macroscopic* internal field in the sample that also can be obtained from the Biot-Savart formula with the molecular currents $\mathbf{j} = c \text{rot} \mathbf{M}$ flowing on the sample's surface, $\mathbf{M} = (g\mu_B S\nu/v_0) \mathbf{e}_z$ inside the sample and $\mathbf{M} = \mathbf{0}$ outside the sample.

In particular, for $\sigma_z(\mathbf{r}) = \sigma_z = \text{const}$ for ellipsoidal samples the integral in Eq. (A12) becomes $4\pi\nu(1 - n^{(z)})\sigma_z \mathbf{e}_z$, where $n^{(z)}$ is the demagnetizing factor. This yields $\mathbf{D}'_z(\mathbf{r}) = D'_{zz} \sigma_z \mathbf{e}_z$, where $D'_{zz} = 4\pi\nu(1/3 - n^{(z)})$. Then Eqs. (A4) and (A5) result in Eq. (14) in the homogeneous case. For a cylinder magnetized with $\sigma_z = \sigma_z(z)$, the field along the symmetry axis is given by Eq. (16).

¹ J. R. Friedman, M. P. Sarachik, J. Tejada, and R. Ziolo, Phys. Rev. Lett. **76**, 3830 (1996).

² J. M. Hernández, X. X. Zhang, F. Luis, J. Bartolomé, J. Tejada, and R. Ziolo, Europhys. Lett. **35**, 301 (1996).

³ L. Thomas, F. Lioni, R. Ballou, D. Gatteschi, R. Sessoli, and B. Barbara, Nature **383**, 145 (1996).

⁴ E. M. Chudnovsky and J. Tejada, *Lectures on Magnetism*

(Rinton Press, Princeton, 2006).

⁵ J. F. Fernández and J. J. Alonso, Phys. Rev. B **62**, 53 (2000).

⁶ X. Martínez Hidalgo, E. M. Chudnovsky, and A. Aharony, Europhys. Lett. **55**, 273 (2001).

⁷ A. Morello, E. L. Mettes, F. Luis, J. F. Fernández, J. Krzystek, G. Aromi, G. Christou, and L. J. de Jongh,

- Phys. Rev. Lett. **90**, 017206 (2003).
- ⁸ M. Evangelisti, F. Luis, E. L. Mettes, N. Aliaga, G. Aromi, J. J. Alonso, G. Christou, and L. J. de Jongh, Phys. Rev. Lett. **93**, 117202 (2004).
- ⁹ F. Luis, J. Campo, J. Gómez, G. J. McIntyre, J. Luzón, and D. Ruiz-Molina, Phys. Rev. Lett. **95**, 227202 (2005).
- ¹⁰ N. V. Prokof'ev and P. C. E. Stamp, Phys. Rev. Lett. **80**, 5794 (1998).
- ¹¹ J. J. Alonso and J. F. Fernández, Phys. Rev. Lett. **87**, 097205 (2001).
- ¹² J. F. Fernández and J. J. Alonso, Phys. Rev. B **72**, 094431 (2005).
- ¹³ A. Cuccoli, A. Fort, A. Rettori, E. Adam, and J. Villain, Eur. Phys. J. B **12**, 39 (1999).
- ¹⁴ D. A. Garanin and R. Schilling, Phys. Rev. B **71**, 184414 (2005).
- ¹⁵ M. Vogelsberger and D. A. Garanin, Phys. Rev. B **73**, 092412 (2006).
- ¹⁶ Y. Suzuki, M. P. Sarachik, E. M. Chudnovsky, S. McHugh, R. Gonzalez-Rubio, N. Avraham, Y. Myasoedov, E. Zeldov, N. E. C. H. Shtrikman, and G. Christou, Phys. Rev. Lett. **95**, 147201 (2005).
- ¹⁷ A. Hernández-Minguez, J. M. Hernández, F. Macia, A. Garcia-Santiago, J. Tejada, P. V. Santos, Phys. Rev. Lett. **95**, 217205 (2005).
- ¹⁸ D. A. Garanin and E. M. Chudnovsky, Phys. Rev. B **76**, 054410 (2007).
- ¹⁹ Kyungwha Park, M. A. Novotny, N. S. Dalal, S. Hill, and P. A. Rikvold, Phys. Rev. B **66**, 144409 (2002).
- ²⁰ L. N. Bulaevskii and V. L. Ginzburg, JETP **18**, 530 (1964).
- ²¹ J. Lajzerowicz and J. J. Niez, J. Phys. (Paris) **40**, L165 (1979).
- ²² J. Kötzler, D. A. Garanin, M. Hartl, and L. Jahn, Phys. Rev. Lett. **71**, 177 (1993).
- ²³ M. Hartl-Malang, J. Kötzler, and D. A. Garanin, Phys. Rev. B **51**, 8974 (1995).
- ²⁴ M. Grahl and J. Kötzler, Z. Phys. B **75**, 527 (1989).
- ²⁵ D. A. Garanin, Physica A **172**, 470 (1991).
- ²⁶ D. A. Garanin, Physica A **178**, 467 (1991).
- ²⁷ E. M. Chudnovsky, D. A. Garanin, and R. Schilling, Phys. Rev. B **72**, 094426 (2005).
- ²⁸ E. M. Chudnovsky and D. A. Garanin, Phys. Rev. Lett. **89**, 157201 (2002).
- ²⁹ E. M. Chudnovsky and D. A. Garanin, Phys. Rev. Lett. **93**, 257205 (2004).
- ³⁰ D. A. Garanin, Phys. Rev. B **68**, 014414 (2003).
- ³¹ D. A. Garanin and R. Schilling, Europhys. Lett. **59**, 7 (2002).